

PERFORMANCE AND MECHANISM OF PHOSPHORUS REMOVAL BY CALCIUM-LOADED CLAY GRANULAR ADSORBENTS

DAI, T. T.¹ – HU, S. F.^{2,3} – CHEN, N.³ – WANG, L.³ – LI, R. Z.³ – LIU, J. F.³ – LI, W.^{3*} – ZHONG, J. Y.^{1*}

¹Jiangxi Provincial Key Laboratory of Water Resources and Environment of Poyang Lake, Jiangxi Provincial Eco-hydraulic Technology Innovation Center of Poyang Lake Basin, Jiangxi Academy of Water Science and Engineering, Nanchang 330029, China

²Jiangxi University of Software Professional Technology, Nanchang 330041, China

³Jiangxi Key Laboratory for Intelligent Monitoring and Integrated Restoration of Watershed Ecosystem, Nanchang Institute of Technology, Nanchang 330099, China

*Corresponding authors

e-mail: liw0791@163.com (W. Li), zjyou666@vip.163.com (J. Y. Zhong)

(Received 17th Oct 2023; accepted 22nd Dec 2023)

Abstract. *In situ* covering and adsorption is a crucial strategy for rapidly reducing the phosphorus content in lake water and suppressing the release of phosphorus from sediments. However, employing rare earth elements or complex modifications of adsorbent materials lead to elevated energy consumption and high costs. Considering the accessibility, affordability, and high ecological safety of calcium hydroxide, red soil, and Calcium-based bentonite, we prepared calcium-red soil-bentonite (CRB) granular adsorbents with different ingredients and investigated their effectiveness. The results showed CRBs with red soil proportions of 60–90% outperformed those with red soil proportions of 0–40%. Specifically, the phosphorus removal efficiency of CRB2 (C:R:B = 1:8:1) exceeded 95%. Also, the adsorption kinetics of CRB2 conformed to pseudo-second-order kinetics and the Elovich model, indicating that CRB2 had a highly heterogeneous surface and that its phosphorus adsorption was chemisorptive. The adsorption isotherm of CRB2 fitted the Langmuir and D-R models, suggesting that the phosphorus adsorption by CRB2 was monolayer chemisorption, with a theoretical maximum adsorption capacity of 17.21 mg/g. Practical application tests revealed that CRB2 effectively lowering phosphorus in the water and suppressing the release of phosphorus from the sediments. These results demonstrate that CRB2 has a potential for large-scale field applications.

Keywords: *modified clay, eutrophication, lake restoration, phosphorus control, adsorption kinetics*

Introduction

Elevated phosphorus (P) content in water bodies as a consequence of human activities is a major factor triggering algal blooms in lakes. In many cases, even with effective control of exogenous phosphorus loading, harmful algal blooms persist due to the release of endogenous phosphorus, and may continue for several decades (Lürling et al., 2016). Hence, effective strategies to control endogenous phosphorus loading in lakes are imperative.

Endogenous phosphorus loading control typically involves *ex situ* and *in situ* control methods. *Ex situ* control often employs sediment dredging, a technology that, while mature and thorough in purifying pollutants, causes substantial sediment disturbance, disrupts lake ecosystems, involves significant engineering efforts, and incurs high costs (Yin et al., 2021). In contrast, *in situ* control, which includes physicochemical remediation and biological remediation, offers ease of construction, less sediment disturbance, and lower treatment costs. Among the physicochemical remediation approaches, metal-based compounds or metal-modified clay minerals are extensively used in lake geoengineering.

The most widely used among these is lanthanum-modified bentonite, yet aluminum, iron, and calcium salts and their modified clay minerals are also frequently utilized (Ma et al., 2022; Yanget al., 2022; Zhang et al., 2019). The addition of these lake geoengineering materials can convert active phosphorus into a stable form of inert phosphorus, thereby inhibiting or reducing the release of sediment phosphorus (Wang and Jiang, 2016).

While iron and aluminum salts can effectively control the active phosphorus content in water bodies and sediments, there are limitations to their use. In the case of iron, it tends to re-release the bound phosphorus under anaerobic conditions. As for the aluminum treatment, it can release toxic substances into the water (such as Al^{3+} and $\text{Al}(\text{OH})_2^+$) when the pH is below 6, thus potentially harming aquatic life (Abell et al., 2020; Vargas and Qi, 2019). In comparison, adsorbent compounds based on rare earth elements have two main disadvantages. First, the crustal abundance of rare earth elements is less than that of other metals like calcium, iron, and aluminum, leading to higher production costs. Second, the zero-point charge of rare earth elements is low, thus limiting the pH range of their use, with a significant decrease in adsorption when the pH exceeds 7 (He et al., 2017). Calcium compounds and calcium compound-modified clay minerals, on the contrary, are cost-effective, environmentally friendly, and exhibit high adsorption efficiency for phosphates, showing a promising application prospect. As early as the 1990s, some North American and European countries used calcium hydroxide and calcium carbonate to treat eutrophic lakes, which significantly reduced water phosphorus and chlorophyll content, and inhibited the release of sediment phosphorus (Dittrich et al., 2011; Prepas et al., 2001). However, the direct use of calcium compounds also led to drastic changes in water pH and produced lightweight calcium-phosphorus flocs that were suspended in the water, causing turbidity. Loading calcium salts on clay might be an effective solution to these problems. Ma et al. (2017) achieved a maximum phosphorus adsorption capacity of 33.52 mg/g and a removal efficiency of 92.82% using calcium oxide-modified bentonite, but the complex modification process limited its large-scale field application. Wu et al. (2020) achieved phosphorus removal efficiency of over 99% by separately mixing calcium hydroxide with bentonite, red soil, and slag, with the maximum phosphorus adsorption capacities reaching 18.42, 20.51, and 41.48 mg/g, respectively. Although the phosphorus removal effect of calcium hydroxide-modified slag was superior to red soil and bentonite, the unstable source and properties of slag also limited its large-scale application. Therefore, it is imperative to conduct further investigations into the potential of using calcium hydroxide-modified red soil and bentonite on a large scale in field applications. While previous studies have mainly used powder forms of these materials, it is important to note that the use of powder may result in turbidity when applied to natural water bodies. To address this issue, we have processed the modified powder into easily applicable granules and have examined their effectiveness in removing phosphorus as well as their mechanism of action. Additionally, we have conducted preliminary testing of their application in natural water, with the aim of providing insights for the large-scale deployment of calcium-loaded clay particles in real-life settings.

Materials and methods

Experimental materials

The clays used as the loading materials of the phosphorus adsorbents in this study were red soil and calcium-based bentonite. Red soil is prevalent in tropical, subtropical, and Mediterranean climate zones, primarily in the southern region of China. This red

soil is rich in iron and aluminum but lacks substantial organic matter and nutrients (Noyma et al., 2016; Peng et al., 2019). Calcium-based bentonite is a layered clay mineral dominated by montmorillonite. It is recognized by its high cation exchange capacity, large specific surface area, wide availability, environmental friendliness, and affordability. Combining the advantages of both types of clay, their mixture may serve as an excellent loading material for phosphorus adsorbents. The red soil used in this study was sourced from the Red Soil Research Institute in Jiangxi Province, China. The soil was prepared by removing impurities such as stones and roots, followed by air-drying and grinding. The soil was then sieved through a 180-mesh screen for further use. Calcium-based bentonite was prepared similarly and procured from Lingshou County Yingbo Mineral Product Processing Factory. Analytical grade calcium hydroxide was obtained from Xilong Scientific Co., Ltd. All experiments were conducted using deionized water with a resistivity of 18.25 $\mu\text{s}/\text{cm}$ (Table 1).

Table 1. Raw material mass ratio of granular adsorbent (%). CRB1–CRB6 represented granules prepared by mixing 10% calcium hydroxide with various proportions of red soil and calcium-based bentonite

	R	B	CRB1	CRB2	CRB3	CRB4	CRB5	CRB6
Calcium hydroxide (C)	0	0	10	10	10	10	10	10
Red soil (R)	100	0	90	80	60	40	20	0
Calcium-based bentonite (B)	0	100	0	10	30	50	70	90

Experimental methods

Preparation of granular adsorbents

Calcium hydroxide was mixed with red soil and Calcium-based bentonite in a granulator (SIMT55, SATEC Electro-Mechanical Technology Co., Ltd.) at set proportions, as shown in Table 1. A suitable amount of pure water was added, and the granulator was run at an appropriate speed to form granules. After the granulation process, particles with diameters between 2 and 3 mm were selected and placed in a constant-temperature air-drying oven to dry for 24 h at 65°C. The resulting granules were then stored in plastic bottles for later use. The proportion of calcium hydroxide was set to 10% based on relevant literature (Wu et al., 2020) and preliminary experimental results. The particles prepared purely from red soil and Calcium-based bentonite were designated as R and B, respectively, while CRB1–CRB6 represented granules prepared by mixing 10% calcium hydroxide with various proportions of red soil and Calcium-based bentonite. For comparison of phosphorus removal effectiveness, a lanthanum-modified bentonite (Phoslock[®], denoted as PL), with a lanthanum element content of 5%, was procured from Jiangsu Jinxin Environmental Engineering Co., Ltd., and examined as a reference.

Structural characterization of granular adsorbents

The morphological characterization of the adsorbents was performed using a scanning electron microscope (SEM, TESCAN MIRA LMS, the Czech Republic). The elemental composition was determined using an SEM-EDS (EDS, Ultim Max Oxford, Instruments United Kingdom). specific surfaces analysis was performed using the

ASAP 2020M model instrument from Quantachrome and then calculated using the BET model. pore structure data were obtained using DFT and BJH models.

Phosphorus adsorption at different dosages of granular adsorbents

Phosphorus solution was prepared using KH_2PO_4 (analytical grade, Xilong Scientific Co., Ltd.), with a concentration of 5 mg/L. The pH of the solution was adjusted to 7 using 0.1 mol/L HCl and NaOH. Various quantities of each type of adsorbent granule (0.025 g, 0.05 g, 0.1 g, 0.15 g, and 0.2 g) were added to 200 mL of the phosphorus solution. Each mixture was agitated at a constant temperature (25°C) for 24 h, after which the mixture was poured onto a 0.45 μm glass fiber filter membrane for filtration, followed by measuring the residual phosphorus concentration in the filtrate. Each experiment was duplicated to ensure the reliability of the results.

Phosphorus adsorption by granular adsorbents at different initial pHs

Phosphorus solution was prepared using KH_2PO_4 , with a concentration of 5 mg/L. The pH of the solution was adjusted sequentially to 3, 5, 7, 9, and 11 using 0.1 mol/L HCl and NaOH. Next, 0.1 g of the adsorbent was added to 200 mL of the phosphorus solution with varying pH values. Each mixture was agitated at a constant temperature (25°C) for 24 h, after which the mixture was poured onto a 0.45 μm glass fiber filter membrane for filtration, followed by measuring the residual phosphorus concentration in the filtrate. Each experiment was replicated to ensure the reliability of the results.

Adsorption kinetics

Phosphorus solution was prepared using KH_2PO_4 with a concentration of 5 mg/L. The pH of the solution was adjusted to 7 using 0.1 mol/L HCl and NaOH. Then, 0.1 g of the adsorbent was introduced into 200 mL of the phosphorus solution, and the mixture was agitated at a constant temperature (25°C) for various time periods (i.e., 0, 0.5, 1, 2, 4, 8, 16, 24, 32, and 48 h). Following each agitation experiment, the mixture was poured onto a 0.45 μm glass fiber filter membrane for filtration, followed by measuring the residual phosphorus concentration in the filtrate. Each experiment was duplicated to ensure the reliability of the results.

Adsorption isotherms

Phosphorus solution was prepared using KH_2PO_4 and adjusted to various concentrations, namely, 0.1, 0.5, 1, 3, 5, 7, 10, 15, and 22 mg/L. The pH of each solution was adjusted to 7 using 0.1 mol/L HCl and NaOH. Next, 0.1 g of the adsorbent was introduced into 200 mL of each phosphorus solution. Each mixture was agitated at a constant temperature (25°C) for 24 h, after which the mixture was poured onto a 0.45 μm glass fiber filter membrane for filtration, followed by measuring the residual phosphorus concentration in the filtrate. Each experiment was replicated to ensure the reliability of the results.

Effectiveness of granular adsorbents in inhibiting the release of sediment phosphorus

Sediments were collected from an aquaculture pond and treated with an appropriate amount of KH_2PO_4 for phosphorus enrichment. The sediment release experiment was conducted indoors using six glass cylinders each with a height of 24 cm and a diameter of 16 cm. Each cylinder was filled with a 6 cm-thick layer of phosphorus-enriched

sediment and covered with 3 L of eutrophic river water (coordinate: 28°41'28.14"N, 116°1'26.48"E), then left undisturbed for three days. Next, the initial total phosphorus content in the water was measured to be 8.34 ± 0.16 mg/L. A control group without granular adsorbent addition was tested, alongside a treatment group in which a granular adsorbent was added at a concentration of 4 g/L. Each group was tested in triplicates, involving measurement of the total phosphorus and orthophosphate phosphorus content in the water at regular time intervals.

Effectiveness of granular adsorbents for phosphorus adsorption in natural waters

The experiment was carried out in the model hall at the Poyang Lake Model Experimental Research Base in Gongqingcheng City, Jiangxi Province, China. Six glass tanks were prepared, each 0.6-m long, 0.5-m wide, and 1.0-m high. Each tank was filled with water from Poyang Lake using a water pump. The water level in each tank was adjusted to a depth of 0.9 m, resulting in a volume of 270 L per tank. The initial total phosphorus content in the water was measured to be 0.537 ± 0.196 mg/L. A control group without granular adsorbent addition was tested, alongside a treatment group in which a granular adsorbent was added at a concentration of 4 g/L. Each group was tested in triplicates, involving measurement of the total phosphorus and orthophosphate phosphorus content in the water at regular time intervals.

Analytical methods

The data obtained from the experiments were organized by Excel 2007 software and plotted by Origin 2021 software. Phosphorus adsorption capacities among treatments were analyzed by one-way analysis of variance (ANOVA). All data were tested for normality and homogeneity before performing comparison. Data were logarithmic transformed to obtain normality and/or homogeneity if they did not meet the basic assumptions. The level of significance for differences among groups was set at $P < 0.05$. Phosphate content was determined by ammonium molybdate spectrophotometry (GB 11893-89). (UV1800PC, obtained from ShangHai jinghua instrument Company, China.)

The adsorbed phosphorus amount at the adsorption equilibrium (Q_e , mg/g) and the percent phosphorus removal (P_p , %) of the granular adsorbent were calculated using *Equations 1* and *2*, respectively:

$$Q_e = \frac{(C_0 - C_e) \cdot V}{m} \quad (\text{Eq.1})$$

$$P_p = \frac{(C_0 - C_e) \cdot 100}{C_0} \quad (\text{Eq.2})$$

where C_0 and C_e are the phosphorus concentration in the solution before and after adsorption ($\text{mg} \cdot \text{L}^{-1}$), respectively, V is the volume of the solution (L), and m is the mass of the adsorbent (mg).

The Langmuir, Freundlich, and Dubinin-Radushkevich (D-R) adsorption isotherm models were used for data fitting, expressed as *Equations 3*, *4*, and *5*. The average free energy E , expressed as *Equation 6*. A fundamental characteristic of the Langmuir isotherm can be expressed by the dimensionless constant separation factor, R_L (also known as the equilibrium parameter), expressed as *Equation 7*, respectively:

$$Q_e = \frac{Q_m K_L C_e}{1 + K_L C_e} \quad (\text{Eq.3})$$

$$Q_e = K_F C_e^{1/n} \quad (\text{Eq.4})$$

$$Q_e = Q_m \exp(-K_{D-R} \varepsilon^2) \quad (\text{Eq.5})$$

$$E = (2K_{D-R})^{-0.5} \quad (\text{Eq.6})$$

$$R_L = 1/(1 + K_L C_0) \quad (\text{Eq.7})$$

where Q_e is the mass of adsorbate adsorbed per unit mass of adsorbent (mg/g), Q_m is the maximum adsorption capacity per unit of the adsorbent for the adsorbate in water (mg/g), K_L is the Langmuir adsorption constant (L/mg), K_F is a constant related to the adsorption affinity in the Freundlich model, K_{D-R} is the D-R constant ($\text{mol}^2 \cdot \text{kJ}^{-2}$), R is the ideal gas constant [$8.314 \text{ J} \cdot (\text{mol} \cdot \text{K})^{-1}$].

The adsorption kinetics data were fitted using the pseudo-first-order, pseudo-second-order, power function, Elovich, and intraparticle diffusion kinetic models, with Equations 8, 9, 10, 11, and 12, respectively:

$$Q_t = Q_e(1 - e^{-k_1 t}) \quad (\text{Eq.8})$$

$$Q_t = \frac{K_2 Q_e^2 t}{1 + K_2 Q_e t} \quad (\text{Eq.9})$$

$$\ln Q_t = \ln(k Q_e) + \left(\frac{1}{m}\right) \ln t \quad (\text{Eq.10})$$

$$Q_t = \frac{1}{\beta} \ln(1 + \alpha \beta t) \quad (\text{Eq.11})$$

$$Q_t = K_{ip} t^{0.5} + C \quad (\text{Eq.12})$$

where t is the reaction time (min), Q_t is the adsorbed amount on the adsorbent surface at time t (mg/g), Q_e is the adsorption amount at equilibrium (also known as the adsorption capacity (mg/g)), k_1 (1/min) and k_2 ($\text{g}/(\text{mg} \cdot \text{min})$) are the rate constants for pseudo-first-order and pseudo-second-order kinetics, respectively, k and m are the reaction rate constants of the power function kinetic model, α ($\text{mg}/\text{g} \cdot \text{h}$) and β (g/mg) are the initial adsorption rate of the adsorbate and the desorption constant in the Elovich kinetic model, respectively, K_{ip} is the intraparticle diffusion constant, and C ($\text{mg} \cdot \text{g}^{-1}$) is the boundary layer thickness.

Results and discussion

Structural characterization of granular adsorbents

Table 2 presents the main chemical compositions of red soil, Calcium-based bentonite, and the CRB series of granular adsorbents. The data revealed that the quantities of aluminum and iron in the red soil (R) surpass those in the Calcium-based

bentonite (B). There is a degree of variation in the aluminum and iron contents in red soil from different regions. For instance, Wu et al. (2020) measured the aluminum and iron contents in red soil (sourced from Changsha County, Hunan Province) as 21.29% and 2.17%, respectively. Liu (2016) indicated that the range of aluminum and iron contents in red soil from various parts of Guangdong Province were 4.4%–11.4% and 3.1%–7.7%, respectively. In the present study, the red soil (collected from Jinxian County, Jiangxi Province) contained 9.99% aluminum and 5.44% iron, while the aluminum and iron contents in the Calcium-based bentonite were merely 5.85% and 1.35%, respectively.

Both red soil and Calcium-based bentonite exhibited relatively low calcium content. The incorporation of calcium hydroxide augmented the calcium levels. In aquatic environments, calcium, iron, and aluminum can precipitate as phosphates, hence their varying levels could potentially affect the phosphorus adsorption capacity of the adsorbents. In the present study, CRB1, CRB2, and CRB3 (with a higher proportion of red soil) contained more aluminum and iron than CRB4, CRB5, and CRB6 (with a higher proportion of Calcium-based bentonite). As each of these materials incorporated 10% of calcium hydroxide, the variance in calcium content was negligible, with an average content of $5.97 \pm 0.47\%$. *Table 2* presents the specific surface area properties of red soil, Calcium-based bentonite, and the CRB series of granular adsorbents. CRB1, CRB2, and CRB3 (with a higher proportion of red soil) contained more specific surface and Micropore volume than CRB4, CRB5, and CRB6 (with a higher proportion of Calcium-based bentonite).

Table 2. Main chemical compositions and specific surface area properties of the adsorption materials

	Na	K	Mg	Si	Al	Fe	Ca	Specific surface	Micropore volume
	(%)							(m ² /g)	(cm ³ /g)
R	0.33	1.66	0.54	21.71	9.99	5.44	0.12	40.67	0.08
B	0.42	0.13	1.22	29.46	5.85	1.35	1.15	60.57	0.13
CRB1	0.08	1.45	0.71	15.21	8.38	4.27	5.28	29.3	0.11
CRB2	0.11	1.01	0.72	17.39	7.69	3.83	5.88	25.65	0.09
CRB3	0.22	1.01	1.00	19.97	7.74	3.52	6.30	27.55	0.1
CRB4	0.10	0.51	1.07	20.64	6.41	2.66	5.61	22.23	0.09
CRB5	0.24	0.35	1.16	22.46	5.55	2.10	6.55	21.18	0.1
CRB6	0.30	0.42	1.21	22.04	5.38	1.96	6.18	17.88	0.01

An SEM analysis of the adsorbent materials was conducted, revealing the surface morphological characteristics of red soil, Calcium-based bentonite, and CRB2, as shown in *Figure 1*. The red soil particles (*Fig. 1a*) exhibited a uniformly blocky structure, while the Calcium-based bentonite particles (*Fig. 1b*) exhibited an extensive, single-layered blocky structure. After calcium hydroxide loading, numerous loose, irregular flocculent structures formed on the surface of CRB1, CRB2, and CRB3 (with 60–90% red soil, *Fig. 1c–e*), potentially augmenting the specific surface area. Meanwhile, the surface materials were evenly distributed and did not exhibit detectable aggregations, which would expose more active sites, thus enhancing the adsorption capacity (Qian et al., 2018). In contrast to CRB1, CRB2, and CRB3, the samples with

50–90% bentonite ratios, i.e., CRB4, CRB5, and CRB6 formed irregular platy and blocky structures (Fig. 1f–h), possibly due to the incorporation of a high proportion of larger-surface-area Calcium-based bentonite.

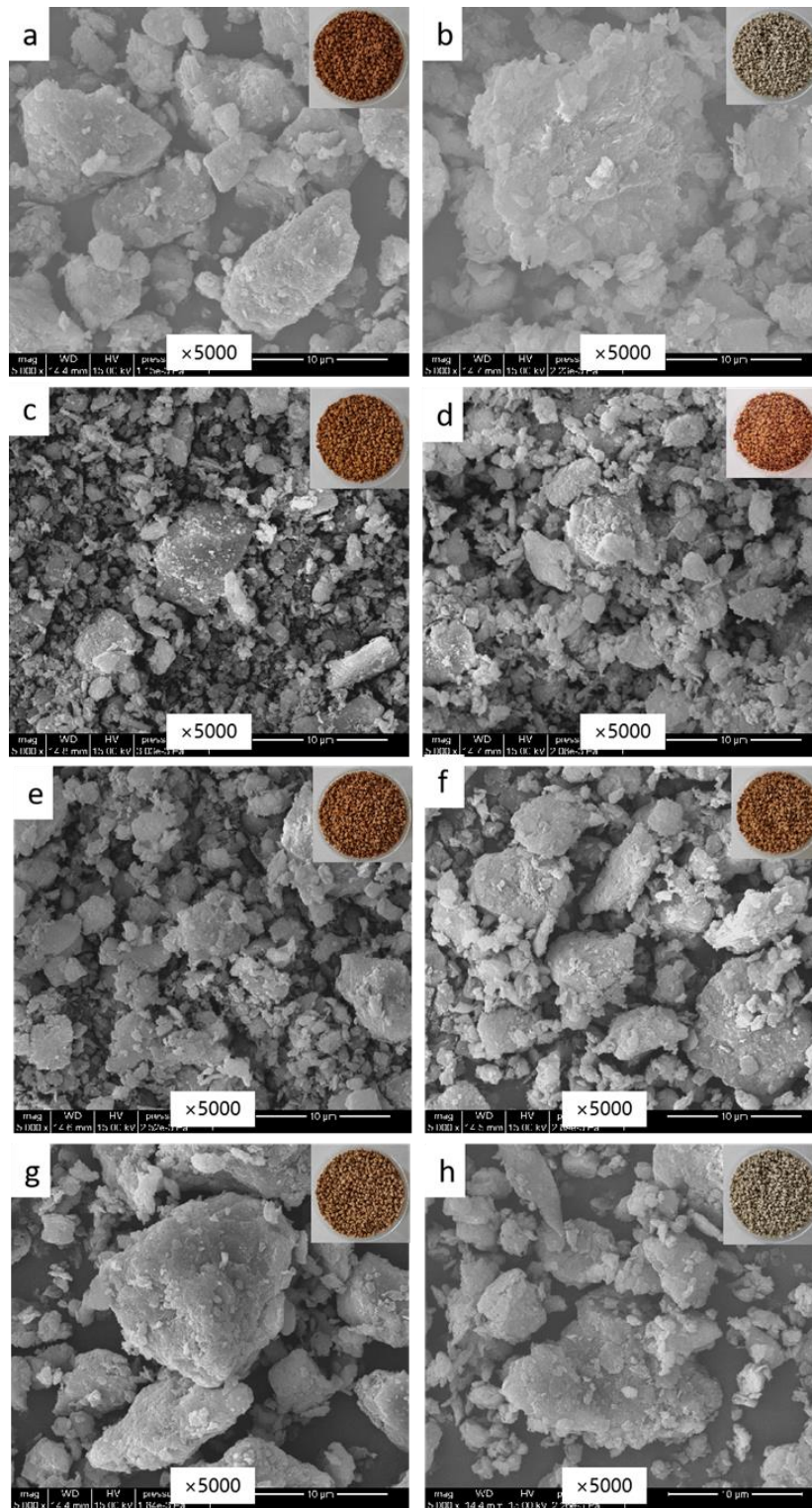


Figure 1. SEM images of (a) red soil, (b) Calcium-based bentonite, (c) CRB1 particles, (d) CRB2 particles, (e) CRB3 particles, (f) CRB4 particles, (g) CRB5 particles, and (h) CRB6 particles

Phosphorus adsorption at different dosages of granular adsorbents

Figure 2 presents phosphorus adsorption capacities at various dosages of granular adsorbents. The phosphorus adsorption capacities exhibited an initial increase followed by a decline as the adsorbent dosage increased. The clay modified with calcium hydroxide demonstrated a substantial enhancement in phosphorus removal compared to red soil and bentonite. At different dosages of adsorbents, CRB1 consistently manifested higher phosphorus adsorption capacities than CRB6 ($P < 0.05$), indicating that the granular adsorbents made from a mixture of calcium hydroxide and red soil outperformed those made from a mixture of calcium hydroxide and bentonite in terms of phosphorus removal performance. Furthermore, our study revealed that when granular adsorbents were made from a mixture of calcium hydroxide, red soil, and bentonite, those comprising 60–90% red soil (i.e., CRB1, CRB2, CRB3) exhibited superior phosphorus removal performance compared to those having 0–40% red soil (i.e., CRB4, CRB5, CRB6) ($P < 0.05$). This is potentially attributable to the higher aluminum and iron contents in red soil compared to bentonite. Among all adsorbents, including PL, CRB2 demonstrated the best phosphorus removal performance at dosages of 0.25–0.5 g/L. At a dosage of 0.25 g/L, CRB2 displayed the maximum phosphorus adsorption capacity of 12.239 mg/g. Increasing the dosage to 0.50 g/L yielded an adsorption capacity of 9.605 mg/g and a percent phosphorus removal of 95.15%.

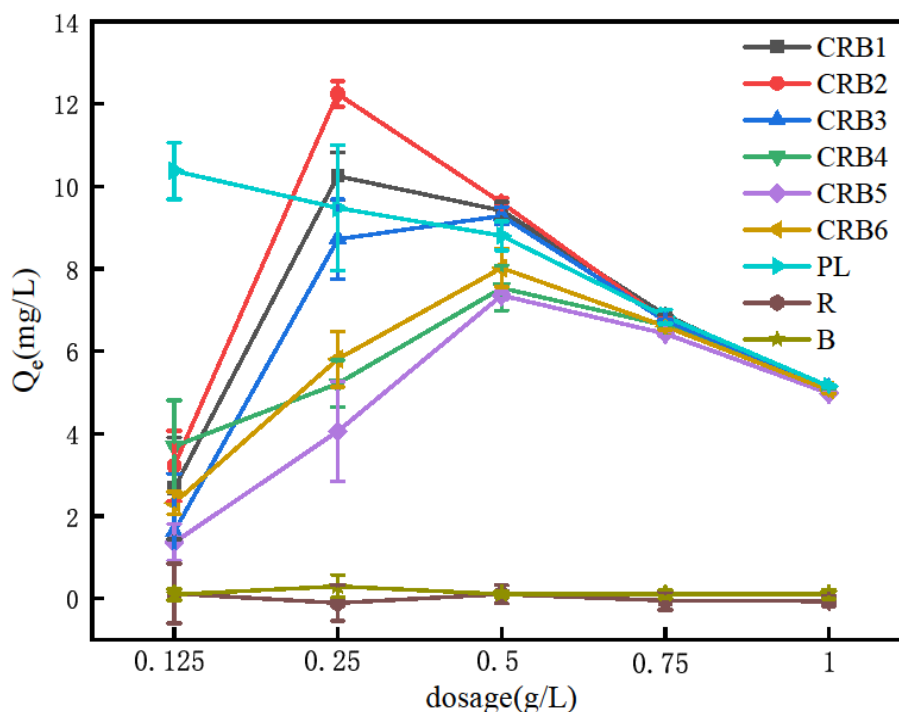


Figure 2. Phosphorus adsorption capacity of granular adsorbents at different dosages. Error bar represent standard deviation

Phosphorus adsorption by granular adsorbents at different initial pHs

Figure 3 illustrates the phosphorus adsorption capacities of granular adsorbents at various initial pH values. When the pH was 3, the phosphorus adsorption capacities of CRB1-6 were all less than 2.2 mg/g, and the removal rate was less than 20%,

demonstrating significantly weaker phosphorus removal performance compared to PL ($P < 0.05$). When the pH was within the range of 5–7, CRB1, CRB2, and CRB3 exhibited higher phosphorus adsorption capacities than PL, CRB4, CRB5, and CRB6, ($P < 0.05$). with CRB2 achieving an adsorbed phosphorus amount up to 9.6 mg/g and a removal rate up to 95.2%. When the solution pH was in the range of 9–11, the adsorbed phosphorus amount of PL dropped sharply, while the phosphorus adsorption capacities of CRB1–6 were all higher than that of PL ($P < 0.05$); meanwhile, CRB1, CRB2, and CRB3 outperformed CRB4, CRB5, and CRB6 ($P < 0.05$) in terms of phosphorus adsorption capacities.

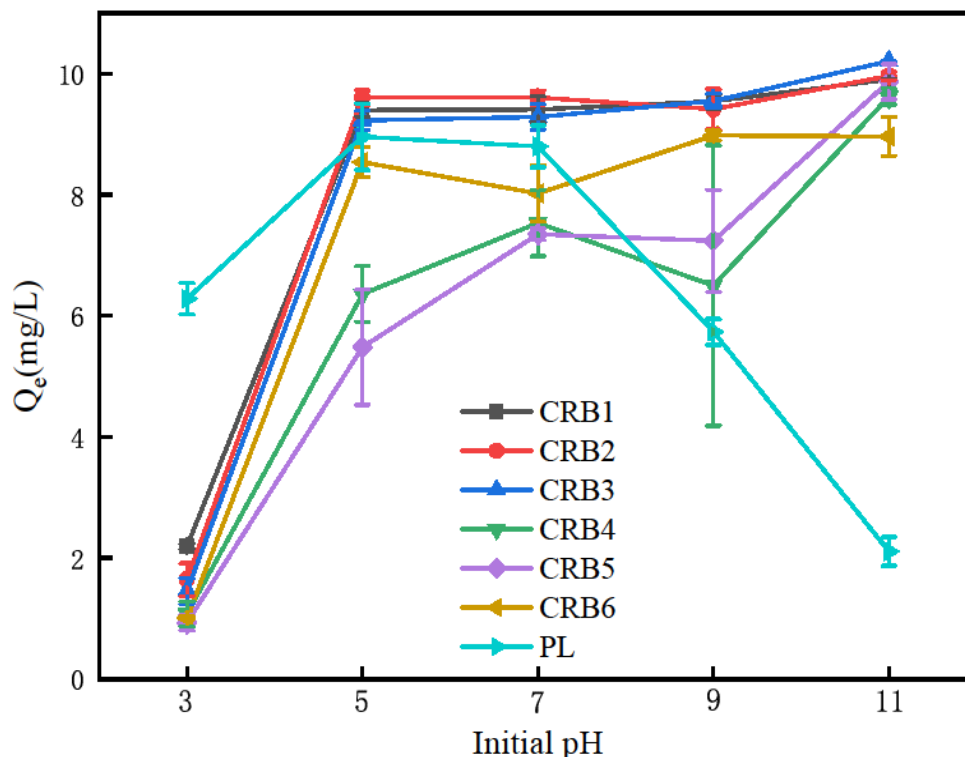


Figure 3. Phosphorus adsorption capacity of granular adsorbents at different initial pH values. Error bar represent standard deviation

Adsorption kinetics

Taking CRB2 as an example, the phosphorus adsorption kinetic data of CRB2 were fitted using the pseudo-first-order, pseudo-second-order, Elovich, power function, and intraparticle diffusion kinetic models, with the results shown in *Figure 4* and *Table 3*. As indicated by the R^2 values, the phosphorus adsorption kinetic data for CRB2 were well-described by the pseudo-second-order ($R^2 = 0.970$), pseudo-first-order ($R^2 = 0.969$), and Elovich ($R^2 = 0.930$) kinetic models, with the fitting performance being significantly superior to that of the power function kinetic model ($R^2 = 0.809$). A maximum adsorption capacity of 11.27 mg/g was obtained from the pseudo-second-order kinetic model, which was close to the experimentally determined maximum adsorption capacity of 10.20 mg/g, indicating that the adsorption process of CRB2 for phosphorus was a chemical process. The Elovich kinetic model suggested that CRB2 had a highly heterogeneous surface with different energy sites.

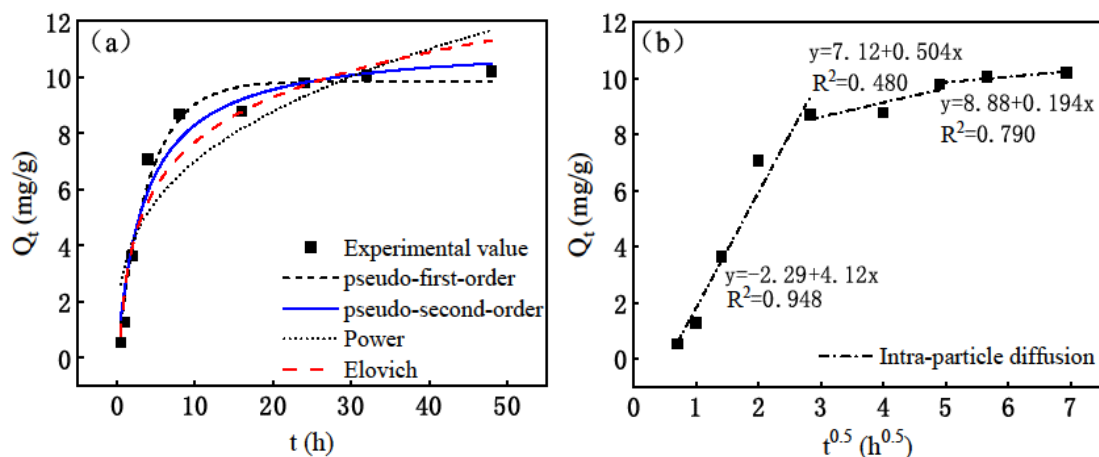


Figure 4. Fitting curves of the phosphorus adsorption on CRB2 using (a) the adsorption kinetic model and (b) the intra-particle diffusion model

Table 3. Kinetic parameters for phosphorus adsorption on CRB2

Pseudo first-order			Pseudo second-order		
Q_m (mg·g ⁻¹)	K_1 (h ⁻¹)	R^2	Q_m (mg·g ⁻¹)	K_2 (h ⁻¹)	R^2
9.78	0.22	0.969	11.27	0.02	0.97
Elovich			Power		
a	b	R^2	$K \cdot Q_e$	m	R^2
6.47	0.43	0.93	3.304	3.065	0.809

Adsorption isotherms

Taking CRB2 as an example, its phosphorus adsorption isotherm data were fitted using the Langmuir, Freundlich, and D-R adsorption isotherm models, with the results presented in *Figure 5* and *Table 4*. As indicated by the R^2 values, the isotherm adsorption data of phosphorus on CRB2 could be adequately described by the Langmuir ($R^2 = 0.875$) and D-R ($R^2 = 0.925$) isotherm models, demonstrating a noticeably superior fitting performance than the Freundlich model ($R^2 = 0.617$). Based on the Langmuir adsorption isotherm model, phosphorus adsorption on CRB2 could be classified as monolayer adsorption. The maximum adsorption capacity of phosphate on CRB2, as per the Langmuir isotherm model, was found to be 17.21 mg/g, which was in close agreement with the maximum experimental value of 16.75 mg/g. This validates the reliability of using the Langmuir isotherm model to predict the maximum adsorption capacity of CRB2. In addition, the calculated R_L values for CRB2 were all within the range of 0–1, with the lower R_L values being evident at higher phosphorus concentrations, indicating that adsorption was more favorable at higher concentrations (Crini et al., 2007). According to the D-R adsorption isotherm model, the E value of CRB2 was calculated to be 15.02 kJ·mol⁻¹, which was higher than 8 kJ·mol⁻¹, implying that the adsorption process of phosphorus in water by CRB2 was a chemisorption process (D’Arcy et al., 2011), in line with the aforementioned result derived from the pseudo-second-order kinetic model.

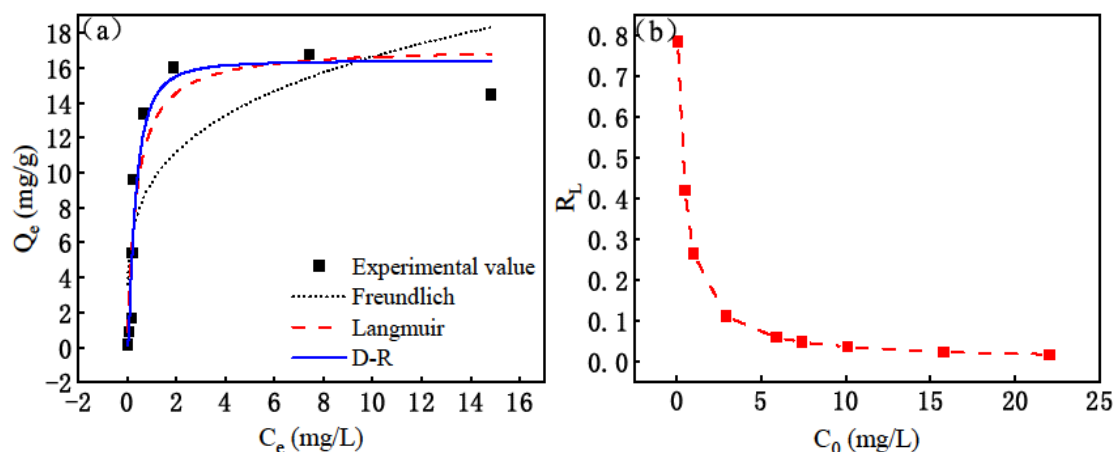


Figure 5. (a) Phosphorous adsorption isotherm and (b) separation factor of Langmuir fitting for CRB2

Table 4. Isothermal adsorption model parameters of CRB2 for phosphorus

Langmuir			Freundlich			D-R			
Q_m ($\text{mg}\cdot\text{g}^{-1}$)	K_L ($\text{L}\cdot\text{mg}^{-1}$)	R^2	K_F ($\text{mg}\cdot\text{g}^{-1}$)	n	R^2	Q_{D-R} ($\text{mmol}\cdot\text{g}^{-1}$)	K_{D-R} ($\text{mol}^2\cdot\text{kJ}^{-2}$)	E ($\text{kJ}\cdot\text{mol}^{-1}$)	R^2
17.21	2.75	0.875	9.44	4.07	0.622	16.41	0.34	15.02	0.925

Table 5 provides an overview of the phosphorus adsorption capacities and optimal pH ranges for various clay-based adsorbents as reported in the literature. The data indicates that while CRB2 has a lower adsorption capacity compared to ACLA, but the latter uses rare earth elements and comes with a higher cost. Generally, conventional iron, aluminum, and rare-earth-modified clay adsorbents reach their maximum phosphorus adsorption levels under acidic and neutral conditions. However, the pH range of urban wastewater typically falls between 6.5–7.3, while eutrophic lakes have a pH of 8–9 (Zamparas and Gianni, 2012). In some water bodies with intense photosynthesis, such as those experiencing harmful algal blooms or excessive growth of submerged plants, the pH can even reach 10. The granular adsorbents developed in this study exhibited significant adsorption capacities under both acidic and alkaline conditions (pH 5-11), making them versatile for a wide range of applications. When used in lakes heavily affected by acid rain, these adsorbents may help neutralize the acidity of the water, thereby preventing damage caused by acid rain. Similarly, in alkaline lake water bodies, these adsorbents may demonstrate substantial adsorption capacities.

Phosphorus removal and control in natural waters

Using CRB2 as an example, the inhibitory effect of CRB2 on phosphorus release from phosphorus-rich sediments is depicted in Figure 6a. Three days after the addition of CRB2, the total phosphorus in the water body sharply dropped from 8.34 ± 0.16 mg/L to 0.39 ± 0.01 mg/L, a decrease of 95.3%. In comparison, the control group depicted an increase of the total phosphorous content by 18.7%, due to the

continuous release of phosphorus from the sediment. After the third day, the total phosphorus in the water bodies of the control group and the CRB2-addition group rose with time. After 28 days, the total phosphorus in the control group increased by 118.3% compared to the initial value, while that in the CRB2-addition group decreased by 67.1% relative to the initial value.

The adsorption performance of CRB2 for phosphorus in natural water bodies is displayed in *Figure 6b*. Although the total phosphorus amounts in the water bodies of both the control group and the CRB2-addition group decreased with time, the removal efficiency (77.5%) and the rate of removal ($0.036 \text{ mg g}^{-1} \text{ d}^{-1}$) in the CRB2-addition group exceeded those in the control group (26.9% and $0.012 \text{ mg g}^{-1} \text{ d}^{-1}$, respectively).

Table 5. Comparison of phosphorous adsorption capacity of clay-based adsorbents

Absorbent	Raw materials	$Q_m / (\text{mg} \cdot \text{g}^{-1})$	pH range	Reference
Phoslock®	Lanthanum chloride and bentonite	10.5	5–7	Haghseresht et al. (2009)
Iron-modified bentonite (Zenith/Fe)	Iron, aluminum, and bentonite	11.2	6–7	Zamparas et al. (2012)
Aluminum-modified zeolite (Z2G1)	Aluminum and zeolite	12.7	5–7	Zamparas and Zacharias (2014)
Aluminum-modified acid-activated bentonite (Al-ABn)	Aluminum and bentonite	12.9	4–7	Pawar et al. (2016)
Attapulgite clay/lanthanum and aluminum (ACLA) composite	Lanthanum, aluminum, and attapulgite clay	34.6	-	Yin et al. (2020)
Calcium-loaded red soil particles (CRB2)	Calcium hydroxide, red soil, and Calcium-based bentonite	17.2	5–11	This study

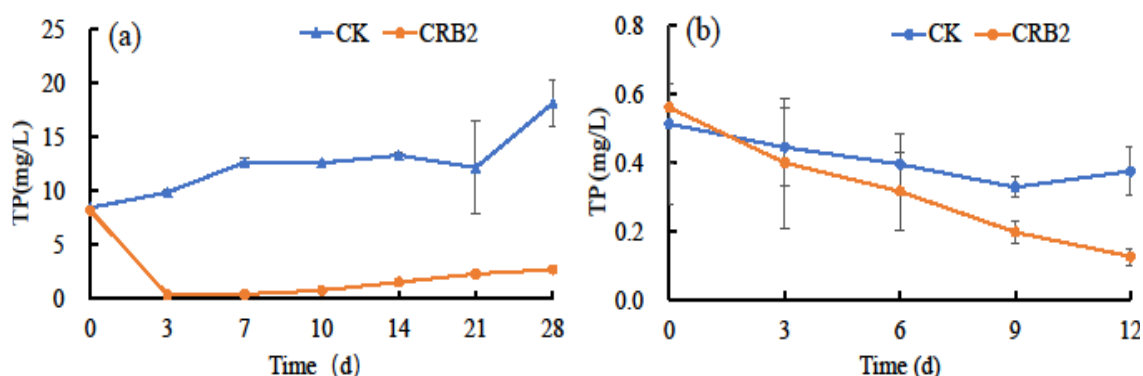


Figure 6. Inhibition of CRB2 on (a) the release of phosphorous from sediment and (b) the adsorption of phosphorous from natural water. Error bar represent standard deviation

Conclusions

We prepared granular adsorbents by uniformly mixing calcium hydroxide with different proportions of red soil and Calcium-based bentonite, and then investigated their phosphorus adsorption performance and mechanisms. The following conclusions were drawn:

(1) When prepared by mixing calcium hydroxide, red soil, and bentonite, the resulting granular adsorbents CRB1, CRB2, and CRB3 (60–90% red soil) contained higher contents of aluminum and iron compared to CRB4, CRB5, and CRB6 (0–40% red soil). Furthermore, the former three adsorbents exhibited more loose and irregular flocculent structures on their surfaces compared to the latter three, which exposed more active sites and improved the adsorption performance.

(2) The granular adsorbents prepared by mixing calcium hydroxide and red soil demonstrated superior phosphorus removal performance compared to those prepared by mixing calcium hydroxide and bentonite. Moreover, the granular adsorbents prepared by mixing calcium hydroxide, red soil, and bentonite revealed improved phosphorous removal performance for the adsorbents with red soil portions of 60–90% (i.e., CRB1, CRB2, and CRB3) compared to those with red soil proportions of 0–40% (i.e., CRB4, CRB5, and CRB6). Among them, the granular adsorbent CRB2—prepared by mixing calcium hydroxide, red soil, and bentonite at a mass ratio of 1:8:1—demonstrated the best phosphorus removal performance.

(3) When exposed to 5 mg/L phosphorus solution at initial pH of 7, CRB2 at a dosage of 0.25 g/L reached its maximum phosphorus adsorption capacity of 12.239 mg/g. Upon increasing the adsorbent dosage to 0.50 g/L, the phosphorus adsorption capacity was 9.605 mg/g, with a phosphorus removal efficiency of 95.15%. The adsorbents CRB1, CRB2, and CRB3 all showed high phosphorus adsorption capacities at pH 5 to 11.

(4) The phosphorus adsorption kinetics of CRB2 conformed to the pseudo-second-order kinetic model and the Elovich kinetic model, indicating that the adsorption process of phosphorus on CRB2 was a combination of surface chemisorption and diffusion, and that CRB2 had a highly heterogeneous surface. The phosphorus adsorption isotherm of CRB2 conformed to the Langmuir and D-R models, implying that CRB2's phosphorus adsorption was monolayer chemisorption. The maximum adsorption capacity for CRB2 calculated from the Langmuir adsorption isotherm model was 17.21 mg/g.

(5) CRB2 could inhibit phosphorus release from phosphorus-rich sediments and reduce phosphorus content in the water body by adsorption. Three days after the addition of CRB2, the total phosphorus in the water body decreased by 95.3%. After 28 days, the total phosphorus in the control group increased by 118.3% compared to the initial value, while that in the CRB2-addition group decreased by 67.1% relative to the initial value. Although the total phosphorus in the water bodies of both the control group and the CRB2-addition group decreased with time, the percent removal (77.5%) and the rate of removal ($0.036 \text{ mg g}^{-1} \text{ d}^{-1}$) in the CRB2-addition group exceeded those in the control group (26.9% and $0.012 \text{ mg g}^{-1} \text{ d}^{-1}$, respectively).

(6) Overall, the calcium-loaded, granular clay adsorbents prepared in this study had the advantages of raw material accessibility, affordability, and simplicity of preparation. Moreover, they exhibited high phosphorus adsorption capacities and a wide pH application range, showing potential for large-scale application in natural water bodies. Further large-scale field trials are needed to evaluate their ecological safety.

Acknowledgments. This work was jointly funded by the National Natural Science Foundation of China (52260026), the “Jiebang Guashuai” Project of the Major Science and Technology Research and Development Program of Jiangxi Province (20213AAG01012), the Key Research and Development Plan of Jiangxi Province (220203BBGL7328), and the Science and Technology Project of Jiangxi Provincial Department of Water Resources (202325ZDKT09). The funders had no role in study design, data collection and analysis, decision to publish, or preparation of the manuscript.

REFERENCES

- [1] Abell, J. M., Özkundakci, D., Hamilton, D. P., Reeves, P. (2020): Restoring shallow lakes impaired by eutrophication: Approaches, outcomes, and challenges. – *Critical Reviews in Environmental Science and Technology* (3): 1-48.
- [2] Crini G., Peindy, H. N., Gimbert, F., Robert, C. (2007): Removal of C. I. Basic Green 4 (Malachite Green) from aqueous solutions by adsorption using cyclodextrin-based adsorbent: Kinetic and equilibrium studies. – *Separation & Purification Technology* 53(1): 97-110.
- [3] D’Arcy, M., Weiss, D., Bluck, M., Vilar, R. (2011): Adsorption kinetics, capacity and mechanism of arsenate and phosphate on a bifunctional TiO₂-Fe₂O₃ bi-composite. – *Journal of Colloid & Interface Science* 364(1): 205-212.
- [4] Dittrich, M., Gabriel, O., Rutzen, C., Koschel, R. (2011): Lake restoration by hypolimnetic Ca(OH)₂ treatment: impact on phosphorus sedimentation and release from sediment. – *Science of the Total Environment* 409(8): 1504-1515.
- [5] Haghseresht, F., Wang, S. B., Do, D. D. (2009): A novel lanthanum-modified bentonite, Phoslock, for phosphate removal from wastewaters. – *Applied Clay Science* (46) 369-375.
- [6] He, Y. H., Lin, H., Dong, Y. B., Wang, L. (2017): Preferable adsorption of phosphate using lanthanum-incorporated porous zeolite: characteristics and mechanism. – *Applied Surface Science* 426: 995-1004.
- [7] Liu, J. F. (2016): Algal Removal and Water Improvement by FeCl₃-Modified Red Soils in Eutrophic Water Bodies. – Jinan University, Guangzhou.
- [8] Lüring, M., Mackay E., Reitzel, K., Spears, B. M. (2016): Editorial – A critical perspective on geo-engineering for eutrophication management in lakes. – *Water Research* 97: 1-10.
- [9] Ma, J. F., Liu, Q., Feng, T. (2017): Adsorption of phosphorus containing wastewater by hydroxyl calcium modified bentonite. – *Journal of Changzhou University (Natural Science Edition)* 29(4): 80-86.
- [10] Ma, X. Y., Yang, P., Zhang, M., Yang, C. H., Yin, H. B. (2022): Advances in researches on phosphorus inactivation materials in Lake sediments. – *Lake Science* 34(1): 1-17.
- [11] Noyma, N. P., Magalhães L., Furtado, L. L., Nunes Teixeira Mucci, M., van Oosterhout, M., Huszar, V. L. M., Marinho, M. M., Lurling, M. (2016): Controlling cyanobacterial blooms through effective flocculation and sedimentation with combined use of flocculants and phosphorus adsorbing natural soil and modified clay. – *Water Research* 97: 26-38.
- [12] Pawar, R., Gupta, P., Lalhmunsiana, Bajaj, C., Lee, S. M. (2016): Al-intercalated acid activated bentonite beads for the removal of aqueous phosphate. – *Science of the Total Environment* (572)1222-1230.
- [13] Peng L., Lei, L. M., Xiao, L. J., Han, B. P. (2019): Cyanobacterial removal by a red soil-based flocculant and its effect on zooplankton: an experiment with deep enclosures in a tropical reservoir in China. – *Environmental Science and Pollution Research* 26(30): 30663-30674.
- [14] Prepas, E., Babin, J., Murphy, T., Chambers, P., Sandland, G., Ghadouani, A., Serediak, M. (2001): Long-term effects of successive Ca(OH)₂ and CaCO₃ treatments on the water quality of two eutrophic hardwater lakes. – *Freshwater Biology* 46(8): 1089-1103.
- [15] Qian C., Yuan, J. G., Zhang, F. Z., Liu, X. Y., Cao, H. Y. (2018): Dynamic adsorption of phosphate by calcium modified bentonite and its regeneration. – *China Water & Wastewater* 34(17): 108-111.
- [16] Tan, K. L., Hameed, B. (2017): Insight into the adsorption kinetics models for the removal of contaminants from aqueous solutions. – *Journal of the Taiwan Institute of Chemical Engineers* 74: 25-48.

- [17] Vargas, K. G., Qi, Z. M. (2019): P immobilizing materials for lake internal loading control: a review towards future developments. – *Critical Reviews in Environmental Science and Technology* 49: 518-552.
- [18] Wang, C. H., Jiang, H. L. (2016): Chemicals used for in situ immobilization to reduce the internal phosphorus loading from lake sediments for eutrophication control. – *Critical Reviews in Environmental Science & Technology* 46: 947-997.
- [19] Wu, L., Chen, X., Liu, F., Li, H. F., Xiao, R. L., Dai, G. J. (2020): Study on phosphorus adsorption characteristics from water by three kinds of $\text{Ca}(\text{OH})_2$ modified materials. – *Water Treatment Technology* 46(3): 50-55 + 61.
- [20] Yang, R., Liu, G., Huang, Y. C., Zhang, Q. Q., Xu, F., Liao, B., Liu, J. (2022): Performance and mechanism of phosphorus removal from micro-polluted water by sulfoaluminate cement. – *Lake Science* 34(3): 828-842.
- [21] Yin, H. B., Yang, C. H., Yang, P., Kaksonen, H., Douglas, B. (2021): Contrasting effects and mode of dredging and in situ adsorbent amendment for the control of sediment internal phosphorus loading in eutrophic lakes. – *Water Research* 189(17): 116644.
- [22] Zamparas, M., Zacharias, I. (2014): Restoration of eutrophic freshwater by managing internal nutrient loads. A review. – *Science of the Total Environment* 496: 551-562.
- [23] Zamparas, M., Gianni, A., Stathi, P., Deligiannakis, Y., Zacharias, I. (2012): Removal of phosphate from natural waters using innovative modified bentonites. – *Applied Clay Science* 62-63: 101-106.
- [24] Zhang, Q. Y., Du, Y. X., Luo, C. Y., Liu, Z. W. (2019): Advances in researches on phosphorus immobilization by lanthanum modified bentonite in lakes and its ecological risk. – *Lake Science* 31(6): 1499-1509.

APPENDIX



Figure A1. Photo of the granulator equipment